引用格式：LI Mi, MA Chengju, LI Dongming, et al. High-sensitivity Fiber-optic Humidity Sensor without Sensitizing Material Modification[J]. Acta Photonica Sinica, 2023, 52(2):0206002
李咪,马成举,李东明,等.无增敏材料修饰的高灵敏度光纤湿度传感器[J].光子学报,2023,52(2):0206002

无增敏材料修饰的高灵敏度光纤湿度传感器

李咪,马成举,李东明,张跃斌,鲍士仟,金嘉升,张垚,刘芊震,
刘洺,张贻歆
(西安石油大学 理学院,西安 710065)

摘　要:设计并制作了一种高灵敏度且制作简单的聚甲基丙烯酸甲酯(Polymethyl Methacrylate,PMMA)微球与单模光纤复合的湿度传感器。该光纤湿度传感器由PMMA微球与单模光纤构成。由于在微球中形成了法布里-珀罗腔,当外界环境湿度升高时,PMMA微球吸收水分子体积膨胀,导致法布里-珀罗腔的腔长增长,使得传感器干涉光谱的波峰(谷)发生红移,从而实现湿度传感。对所制作传感器的湿度响应、稳定性和重复性等进行了实验研究,实验结果表明:在30%~80%湿度范围内,该湿度传感器的灵敏度达173.36 pm/%RH,波长漂移随相对湿度变化呈良好的线性关系,其线性度达0.992 26,且具有良好的稳定性和重复性。该PMMA微球与单模光纤复合的湿度传感器具有灵敏度高、结构简单、无需镀膜且易于制作的优点。

关键词:光纤传感器;聚甲基丙烯酸甲酯;单模光纤;法布里-珀罗腔;相对湿度
中图分类号:TN253　　**文献标识码**:A　　**doi**:10.3788/gzxb20235202.0206002

0　引言

持续监测环境相对湿度(Relative Humidity,RH)的变化,在环境安全[1]、农业[2]、电力[3]和医药工程[4]等领域至关重要。湿度传感器的测湿范围、机械性能、抗电磁辐射性等性能参数,直接决定着湿度传感器能否满足实际应用的需求。目前,常见的光纤湿度传感器根据传感机理的不同,主要有干涉型光纤湿度传感器、吸收型光纤湿度传感器、倏逝波型光纤湿度传感器和光纤光栅湿度传感器等。其中,基于法布里-珀罗(Fabry-Pérot,F-P)的光纤传感器具有结构简单、成本低和灵敏度高等优势,在温度[5]、湿度[6]、压力[7]和折射率[8]等传感领域中受到科研人员的关注。例如,2013年,SU D等[9]提出了一种将聚乙烯醇(Polyvinyl Alcohol,PVA)湿敏材料涂覆在单模光纤(Single Mode Fiber,SMF)端面所构成的F-P结构,用来实现湿度传感,其湿度测量范围为7%RH~91.2%RH,灵敏度为70 pm/%RH。2019年,ZHAO Y等[10]报道将湿敏材料石墨烯量子点(Graphene Quantum Dots,GQDs)聚乙烯醇填充到空芯毛细管的传感器结构,在13.47%RH~81.34 %RH范围内实现了灵敏度为117.25 pm/%RH的湿度传感,同时波长漂移和湿度变化具有良好的线性关系。与基于其它原理的光纤湿度传感器相比,基于法布里-珀罗干涉仪(Fabry-Pérot Interferometer,FPI)的光纤湿度传感器具有易于制作、可逆性好和可重复性高等优点,备受科研人员的关注。

现有的光纤传感器多数采用石英光纤,由于普通单模光纤芯较脆弱且灵活性差,这就需要研究新型的材料和结构,实现湿度检测。与石英光纤相比,聚合物光纤(Polymer Optical Fiber,POF)因具有柔韧性好、低成本、导光能力强等特有的优点而受到科研人员的青睐。近年来,POF已被应用于温湿度[11]、折射率[12]、液位[13]和生物[14]等传感器研究。例如,2014年,英国阿斯顿大学[15]报道了一种基于POF的光纤布拉格光栅

基金项目:陕西省重点研发计划(No. 2018GY-062),西安石油大学创新与实践能力培养项目(No. YCS20213213)
第一作者:李咪,limitj@126.com
通讯作者:马成举,chengjuma@xsyu.edu.cn
收稿日期:2022-07-20;**录用日期**:2022-11-29

(Fiber Bragg Grating,FBG)湿度传感器,利用聚甲基丙烯酸甲酯(Polymethyl Methacrylate,PMMA)随湿度的增加而体积膨胀的机理,以及FBG对膨胀应力的响应,实现了湿度传感。为了实现温湿度同时测量,2019年,OLIVEIRA R等[16]提出一种双光纤传感器,该系统由紫外胶(NOA78)制成的F-P与微聚合物光纤(Microstructured Polymer Optical Fiber,mPOF)布拉格光栅相结合构成,用来同时检测环境温湿度。实验结果表明,该系统对温度和湿度测量误差分别低于0.2 ℃和0.2%RH。2021年,中北大学HU Y J等[17]设计了一种基于表面等离子体共振(Surface Plasmon Resonance,SPR)效应和倏逝波损耗的mPOF湿度传感器。利用磁控溅射法在mPOF表面得到50 nm的金层,再将浓度为0.5 %的琼脂糖涂敷在金膜表面,从而产生金层-琼脂糖层界面的SPR效应。在湿度为20%~80%时,灵敏度为0.595 μW/%RH。对于绝大多数光纤湿度传感器来说,需要复杂的湿敏材料涂敷和微结构制作,这增加了制作过程的成本和复杂性。因此,制作一种结构简单、灵敏度高、稳定性好以及可重复使用的湿度传感器具有重要的研究意义和应用价值。

本文设计并制备了一种基于PMMA微球与单模光纤复合的湿度传感器。该传感器是利用电烙铁对PMMA聚合物光纤进行加热,在单模光纤端面形成一个PMMA微球,构成FPI结构。由于PMMA材料自身对湿度敏感,湿度的变化会导致FPI腔长发生改变。实验中,通过监测传感器的反射光谱,实现了湿度灵敏度为176.05 pm/%RH,线性度可达0.992 26的湿度传感。所提出的传感器具有制备容易、灵敏度高、稳定性好和重复性强等优点。

1 传感器的结构、制作及湿度传感原理

所设计的光纤湿度传感器的结构示意如图1(a),该传感器由SMF和熔融POF形成的PMMA微球构成。实验中所使用的SMF是由长飞公司生产,其包层直径为125 μm,纤芯直径为8.2 μm。POF是森沃光电科技有限公司生产的阶跃型聚合物光纤,其芯层直径为980 μm,折射率为1.49;包层直径为20 μm,折射率为1.41。

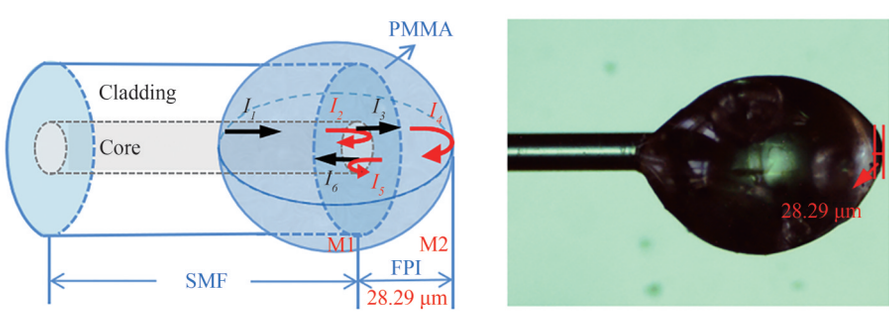

(a) Schematic diagram of structure (b) Microscopic photo

图1 传感器结构

Fig. 1 Structure of sensor

由于聚合物光纤材料的熔点为70 ℃,在实验中,当电烙铁加热至70 ℃左右时,非常容易将其加热到熔融状态。具体的流程制备为:首先,取一段SMF用剥纤钳剥去涂覆层,经酒精反复擦洗后,使用光纤切刀切割得到良好的光纤反射端面。处理好的SMF一端被固定在一定高度的平台上,并将另一端连接到SM125解调仪用来实时监测反射光谱。然后,取长度约为4 mm的POF用镊子夹持,当电烙铁加热温度高达聚合物光纤熔点后,将其置于POF下1 cm处,使POF轻微附着在单模光纤上。最后,在POF周围需要慢慢旋转加热源(即电烙铁),以确保POF可以被均匀加热。当结构冷却后,使PMMA微球紧紧固定于单模光纤端面。需要注意的是,在加热过程中,由于POF的熔融温度范围较小,所以通过加热源的温度以及光纤与加热源的距离,控制好加热的温度,就可以很好地调节微球的形状与尺寸,以及PMMA薄膜的长度(即F-P腔长)。实验中采用电烙铁加热法,相比酒精灯加热法,电烙铁能够提供稳定的加热源,且安全系数高。经过多次尝试后,积累经验,并通过解调仪实时监测反射光谱,就可以提高制作的成功率。从而,在单模光纤端面上成功地熔融一个PMMA微球,光纤F-P传感探头结构的光学显微图如图1(b),F-P腔长L为28.29 μm。

光在该传感器结构中的传输过程:当一束光强为I_1的光从单模光纤一端传输到M1界面(SMF/PMMA)时,由于M1界面两侧折射率的不同而产生了菲涅尔反射,一部分光强为I_2光束会被反射回SMF中,剩余部

分的光（透射光强I_3）继续进入到微球中。PMMA和空气的交界面（M2）被看作第二个反射面，在M2界面也发生反射现象。于是，当光强为I_4的反射光又传输回M1界面时，一部分光（I_6）重新透射到单模光纤纤芯，同时，一小部分光在FP腔内有二次反射（I_5）并且反射光强很低。因此，M1界面的反射光强I_2和透射光强I_6叠加产生双光束干涉，从而形成法布里-珀罗干涉。

由光的干涉理论可知，干涉光的总光强可以表示为[18]

$$I=I_2+I_6+2\sqrt{I_2I_6}\cos\left(\frac{4\pi nL}{\lambda}+\varphi_0\right) \tag{1}$$

式中，I_2和I_6分别为两束反射光的光强，φ_0为初始相位，λ为工作波长，n和L分别为F-P腔有效折射率和长度。当相位差满足$\frac{4\pi nL}{\lambda_m}=2m\pi$（$m$为正整数）时，反射谱出现干涉峰，其波长表示为

$$\lambda_m=\frac{2nL}{m} \tag{2}$$

由式（1）和（2）可得，两个相邻波峰的波长间隔即自由光谱范围（Free Spectrum Range，FSR）为

$$\mathrm{FSR}=\lambda_m-\lambda_{m+1}\approx\frac{\lambda^2}{2nL} \tag{3}$$

当外界湿度上升（或降低）时，PMMA吸收水分子发生体积膨胀（或收缩）。因此，F-P腔的腔长发生改变，同时PMMA折射率增大，导致对光纤中传输的光波信号产生影响，从而实现对相对湿度的感知。随着湿度增加，折射率增大和PMMA长度增长，波谷向长波长方向移动（即红移），灵敏度可以表示为

$$\frac{\Delta\lambda}{\Delta\mathrm{RH}}=\lambda\left(\frac{1}{n}\frac{\mathrm{d}n}{\mathrm{dRH}}+\frac{1}{L}\frac{\mathrm{d}L}{\mathrm{dRH}}\right) \tag{4}$$

根据式（4），可以看出传感器灵敏度与腔长L成反比。当F-P腔长越短时，传感器灵敏度越高。即PMMA微球越小，传感器的灵敏度越高。

2 湿度传感响应研究

实验中，采用解调仪（SM125，MOI，USA）作为输入光源和解调装置，入射光波波长范围为1 520～1 580 nm，分辨率为1 pm，将电脑和解调仪连接，用以观察和记录解调的反射光谱。传感湿度测量系统装置示意如图2。

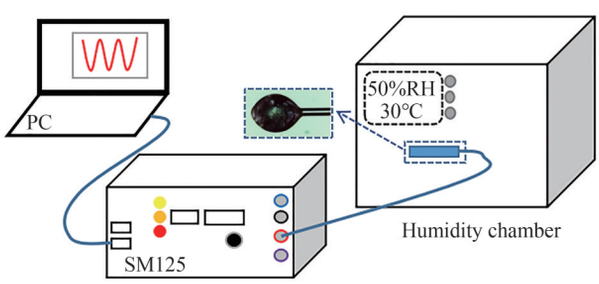

图2 传感器湿度测量系统示意

Fig. 2 Schematic of the sensor humidity measurement system

传感器置于密闭的湿度箱内。记录的室温下传感器的反射光谱如图3（a），干涉光谱的对比度约为23.8 dBm，FSR约为29 nm。为进一步分析干涉现象，对干涉谱进行信号解调处理，通过快速傅里叶变换（Fast Fourier Transform，FFT）得到反射光谱的幅频特性曲线。由光速公式$v=c/\lambda$，可将干涉信号从波长域转换到频率域，把自变量为光频率v的干涉谱作FFT算法后，得到幅频特性曲线[19]。在原光谱的空间频谱中得到峰值处的光谱频率。图3（b）是其空间频谱图，相对应FFT的主频率为$1/\mathrm{FSR}=0.033\ \mathrm{nm}^{-1}$，由式（3）得到FSR的理论值约为28.50 nm，与实测光谱的FSR吻合。由图可知，存在一个明显的主峰和两个次峰，这两个次峰是主峰的频率倍数，这说明传感器的干涉谱主要是由SMF/PMMA和PMMA/空气界面反射光之间的干涉决定的。

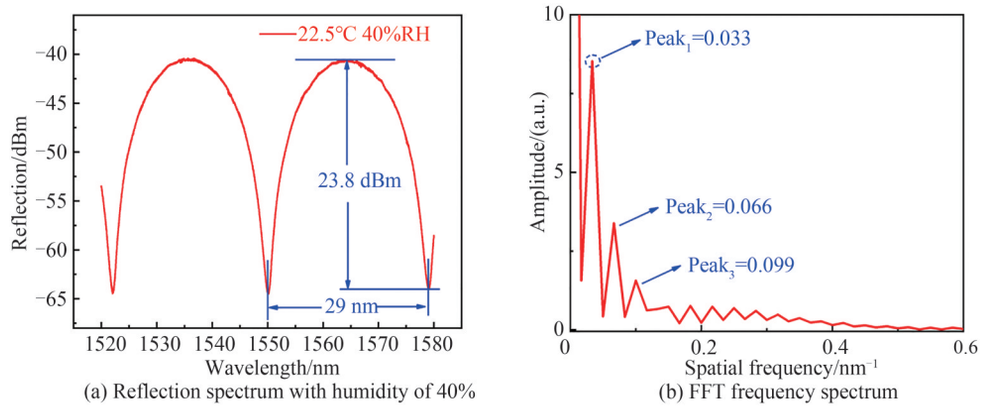

(a) Reflection spectrum with humidity of 40%　(b) FFT frequency spectrum

图 3　传感器光谱

Fig. 3　The spectrum of sensors

3　传感器温湿度的响应测试

3.1　传感器湿度响应测试

首先，对微球型传感结构的湿度特性进行了实验研究。其中，湿度环境由密闭箱内盛有水溶液的烧杯来提供，置于湿度箱的电子湿度计用来标定相对湿度。实验中，控制湿度箱的温度稳定（温度约为 22.5 ℃），相对湿度从 30%RH 逐步上升到 80%RH，每间隔 10%RH 记录一次光谱数据，不同湿度的反射光谱如图 4(a)。随着湿度增加，更多的水分子被 PMMA 微球吸收，导致其密度变高，折射率增大，从而导致波谷向长波长方向移动（即红移），当相对湿度从 30%RH 变化到 80%RH 时，反射谱的红移达到 9.38 nm。由实验测量数据可得到相对湿度与反射谱波长的拟合关系，如图 4(b)，反射光谱波长与湿度的变化呈线性关系，湿度灵敏度为 176.05 pm/%RH，线性拟合度为 0.992 26。

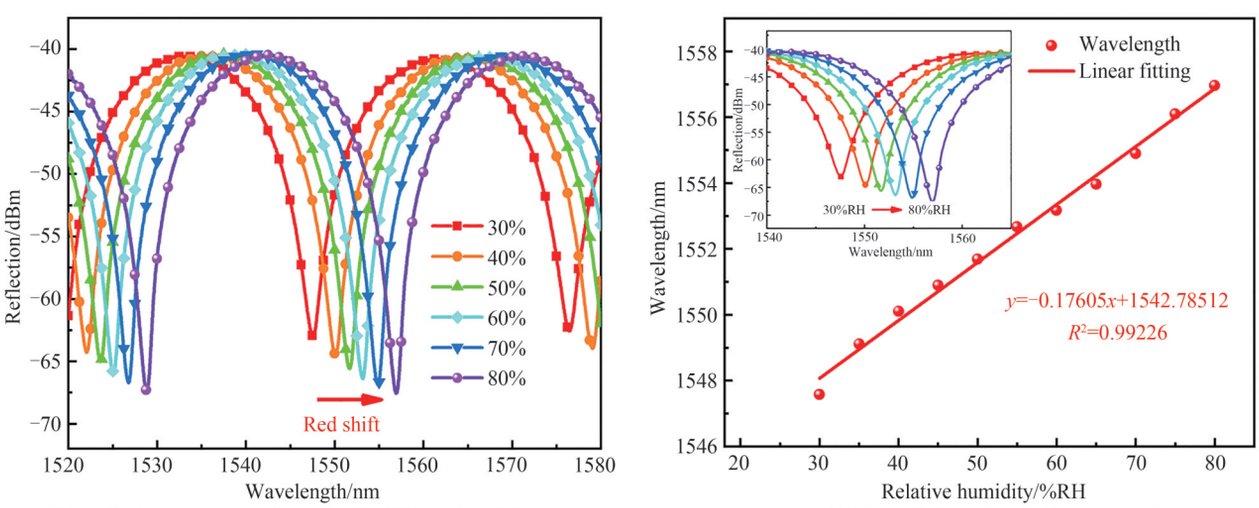

(a) Reflection spectrum of sensor with different humidity　(b) Linear fitting relationship between the relative humidity and wavelength

图 4　传感器湿度响应

Fig. 4　Humidity response of sensor

3.2　传感器温度响应测试

对于光纤湿度传感器，温度串扰是必须要考虑的问题。在温度传感实验研究中，将所制作的传感器放入精度为 1 ℃的温度箱（NBD-M1200-10IC，NOBODY. China）中，温度从 30 ℃逐渐升至 65 ℃，待温箱的温度稳定后，每间隔 5 ℃监测一次反射谱，记录了 8 组温度实验数据。

由于环境温度发生变化时，PMMA 材料的折射率和体积都会发生变化，从而引起反射光谱的波长偏移，影响湿度传感性能。在不同温度下，传感器的波长与温度的拟合关系如图 5。当温度为 35 ℃～65 ℃时，传感器的

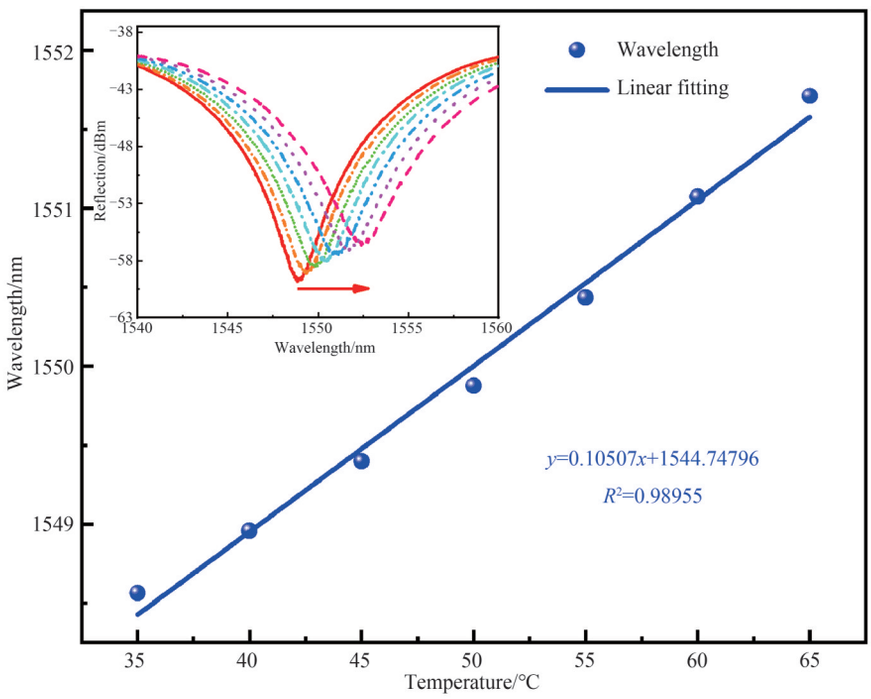

图 5　在 30 ℃～65 ℃下波长与温度的拟合关系

Fig. 5　Linear fitting relationship between the temperature and wavelength when temperature ranges from 30 ℃ to 65 ℃

反射谱红移约 3.15 nm,传感器的温度灵敏度为 105.07 pm/℃,线性拟合度为 0.989 55。可以看出 PMMA 材料对温度也敏感,在后续的研究中,通过在该传感器中级联 FBG,解决该湿度传感器的温湿度交叉敏感的问题。

4　传感器稳定性和重复性测试

4.1　传感器稳定性测试

为了衡量所制作传感器的稳定性,对其进行实验测试。将湿度传感器放置在温度恒定(22.5 ℃)的密闭箱内,在不同时间节点下,分别选择监测了 RH 为 33% 和 38%(低湿度环境)的反射谱,并持续监测 1 h。当传感器的反射光谱达到稳定时,开始记录透射谱,此后间隔 10 min 记录一次反射谱,总共记录 7 组数据。图 6(a)为 60 min 内传感器的反射光谱图,插图为波谷处的局部放大图。由实验图可明显地看出 1 h 内湿度传感器的反

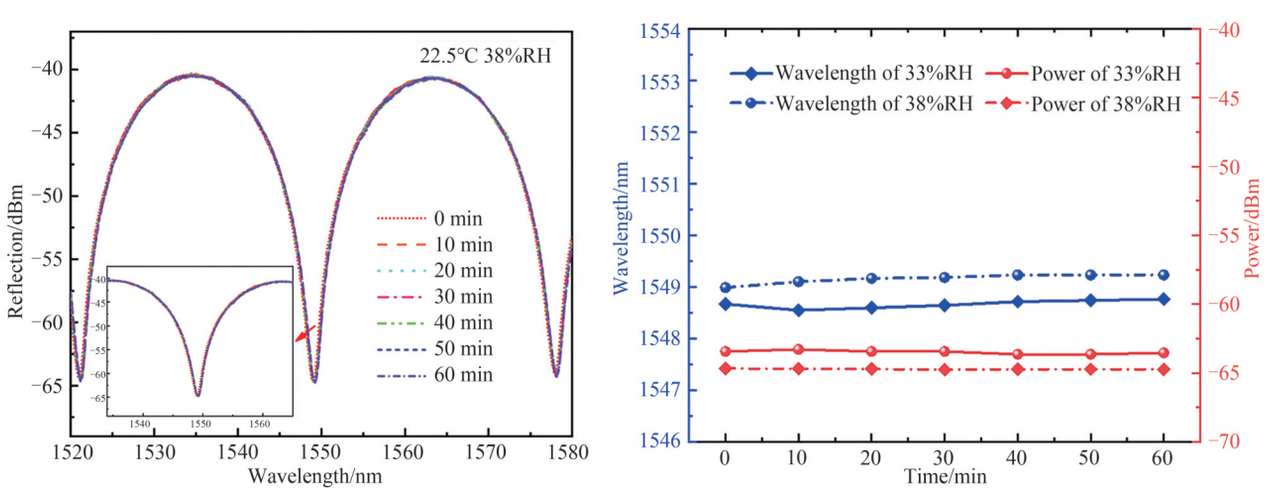

(a) Reflection spectrum of the sensor at humidity of 38%, temperature of 22.5 ℃, inset is partially enlarged view of the dip

(b) When humidity of 33% and 38%, power and wavelength changes of the reflection spectrum with time

图 6　传感器的稳定性测试

Fig. 6　Stability test of the sensor

射光谱基本没有变化。图6(b)为随时间的变化，相对湿度33%RH和38%RH下，传感器反射谱的波谷功率和波长的变化。从图中看出，在60 min内，随着时间的流逝，不同湿度环境下波谷的漂移很小，性能十分稳定，最大偏差分别为0.08 nm和0.09 nm。由此表明所提出的传感器在长时间工作状态下可以保持良好的稳定性。

4.2 传感器重复性测试

进一步研究了该传感器的重复性。在三个不同的时间点下(实验温度依次约为22.5 ℃、23.6 ℃和33.5 ℃)，对所提出的传感器进行三次湿度测量的重复性测试，三次实验的线性拟合结果如图7。三次重复实验中波长漂移量存在较小偏差，灵敏度分别为176.05 pm/%RH、170.35 pm/%RH和173.68 pm/%RH，线性拟合度分别为0.992 26、0.991 69和0.992 05。实验中的测量误差导致了湿度灵敏度的极小差值。三组数据灵敏度的平均值为173.36 pm/%RH，即所提出传感器的灵敏度为173.36 pm/%RH。由此表明该传感器在湿度测量中具有良好的可重复性。此外，环境温度也影响湿度的测量，因此在实验中应严格控制温度的变化，尽量在温度恒定下进行湿度的测量。

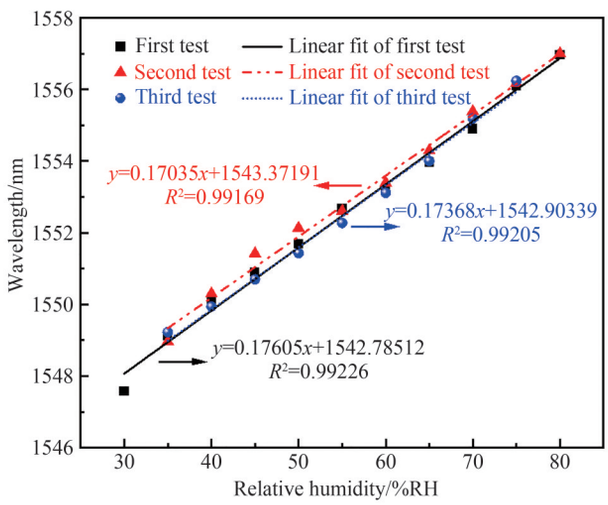

图7 重复性测试

Fig. 7 Repeatability test of the sensor

表1为所设计的传感器与其它类型光纤湿度传感器的性能比较。可以看出，所设计的湿度传感器在灵敏度、稳定性以及线性度等方面都具有较好的表现，且表1中所列出的其它湿度传感器大都涂敷或填充了湿敏材料。比如，文献[25]的湿度灵敏度较高，并涂敷透明质酸(Hyaluronic Acid，HA)/PVA复合膜。而本文所制作的传感器实现了不需要任何涂敷湿敏材料的方法来实现湿度传感，不仅节约成本，而且降低了制作

表1 光纤湿度传感器的性能比较

Table 1 Performance comparison of the fiber-optic humidity sensors

Type	Humidity sensitivity material	RH range/%RH	Sensitivitypm/%RH	Ref.
Mach-Zehnder Interferometer (MZI)	Chitosan	10～90	119.6	[20]
FPI	GQDs-PVA	13.47～81.34	117.25	[10]
Michelson Interferometer (MI)	Methylcellulose (MC)	55～85	133	[21]
Mismatching Fused Mach-Zehnder Interferometric (MFMZI)	No coating	Beyond～87.5%RH	166.7	[22]
MZI and FPI	GQDs-PVA	27.83～76.1	132	[23]
Whispering-gallery Mode (WGM) resonator	No coating	30～90	54	[24]
Dual FPIs	PVA Polydimethylsiloxane (PDMS)	20～45	128 38	[25]
FPI	HA and PVA	35～85	233	[26]
POF FPI	No coating	30～80	173.36	Our work

难度。因此,所提出的光纤湿度传感器的综合性能具有较大的优势。

5 结论

本文提出并制作了一种基于PMMA微球与单模光纤复合的湿度传感器。该传感器通过在单模光纤尖端熔融PMMA微球构成F-P腔,形成光纤湿度传感器。对该传感器的湿度响应特性进行了研究,实验结果表明,传感器在30%~80%湿度范围内,灵敏度达到176.05 pm/%RH,线性拟合度为0.992 26;在35 ℃~65 ℃温度范围内,传感器的温度灵敏度为105.07 pm/℃,线性拟合度为0.989 55。稳定性实验测试表明,不同环境湿度下,反射谱波长漂移的最大偏差分别为0.08 nm和0.09 nm;重复性实验测试表明,平均湿度灵敏度高达173.36 pm/%RH。所设计的湿度传感器具有易于制作、无需镀膜、低成本、灵敏度高、稳定性好、可重复性强等特点。

参考文献

[1] YAN Guofeng, WANG Binhao, MA Guiying, et al. Fiber-optic acetylene gas sensor based on microstructured optical fiber bragg gratings[J]. IEEE Photonics Technology Letters, 2011, 23(21): 1588-1590.

[2] ZHAO Lin, WANG Jiqiang, LI Zhen. Quasi-distributed fiber optic temperature and humidity sensor system for monitoring of grain storage in granaries[J]. IEEE Sensors Journal, 2020, 20(16): 9226-9233.

[3] KIM H J, SHIN H Y, PYEON C H, et al. Fiber-optic humidity sensor system for the monitoring and detection of coolant leakage in nuclear power plants[J]. Nuclear Engineering and Technology, 2020, 52(8): 1689-1696.

[4] JEONG W, SONG J, BAE J, et al. Breathable nanomesh humidity sensor for real-time skin humidity monitoring[J]. ACS Applied Materials & Interfaces, 2019, 11(47): 44758-44763.

[5] CAI Lizou, QIN Yali, CAI Xiaolei, et al. Sensitization method of Fabry-Pérot temperature sensor based on vernier principle[J]. Laser & Optoelectronics Progress, 2021, 58(11): 1106004.
蔡礼邹, 覃亚丽, 蔡小磊, 等. 基于游标原理的法布里-珀罗温度传感器的增敏方法[J]. 激光与光电子学进展, 2021, 58(11): 1106004.

[6] LI Cheng, YU Xiyu, ZHOU Wei, et al. Ultrafast miniature fiber-tip Fabry-Pérot humidity sensor with thin graphene oxide diaphragm[J]. Optics Letters, 2018, 43(19): 4719-4722.

[7] ZHANG Yutong, JIANG Yi, CUI Yang, et al. Research on the micro optical fiber Fabry-Pérot ultra-low temperature pressure sensor[J]. Acta Photonica Sinica, 2022, 51(5): 0551315.
张雨彤, 江毅, 崔洋, 等. 微纳光纤Fabry-Pérot超低温压力传感器研究[J]. 光子学报, 2022, 51(5): 0551315.

[8] SU Yudong, WEI Yong, WU Ping, et al. Step-index multimode fiber cladding surface plasma resonance sensor[J]. Optics and Precision Engineering, 2019, 27(12): 2525-2533.
苏于东, 魏勇, 吴萍, 等. 阶跃折射率多模光纤包层等离子体共振传感器[J]. 光学精密工程, 2019, 27(12): 2525-2533.

[9] SU Dan, QIAO Xueguang, RONG Qiangzhou, et al. A fiber Fabry-Pérot interferometer based on a PVA coating for humidity measurement[J]. Optics Communications, 2013, 311: 107-110.

[10] ZHAO Yong, TONG Ruijie, CHEN Maoqing, et al. Relative humidity sensor based on hollow core fiber filled with GQDs-PVA[J]. Sensors and Actuators B: Chemical, 2019, 284: 96-102.

[11] ZHONG Nainbing, XIN Xin, LIU Huimin, et al. Plastic optical fiber sensor for temperature-independent high-sensitivity detection of humidity[J]. Applied Optics, 2020, 59(19): 5708-5713.

[12] OLIVEIRA R, BILRO L, NOGUEIRA R, et al. Multiparameter POF sensing based on multimode interference and fiber bragg grating[J]. Journal of Lightwave Technology, 2017, 35(1): 3-9.

[13] CHEN Junlian, LI Linyang, XIN Xin, et al. Reflective spiral plastic fiber-optic sensor for accurate detection of liquid level[J]. Acta Optica Sinica, 2021, 42(1): 0106005.
陈俊琏, 李林洋, 辛鑫, 等. 准确测量液位的反射式螺旋塑料光纤传感器[J]. 光学学报, 2021, 42(1): 0106005.

[14] YAO Baicheng, WEBB D J, POSPORI A, et al. Graphene-based D-shaped polymer FBG for highly sensitive erythrocyte detection[J]. IEEE Photonics Technology Letters, 2015, 27(22): 2399-2402.

[15] ZHANG Wei, WEBB D J. Humidity responsivity of poly(methacrylate)-based optical fiber Bragg grating sensors[J]. Optics Letters, 2014, 39(10): 3026-3029.

[16] OLIVEIRA R, BILRO L, NOGUEIRA R, et al. Simultaneous detection of humidity and temperature through an adhesive based Fabry-Pérot cavity combined with polymer fiber Bragg grating[J]. Optics and Lasers in Engineering, 2019, 114: 37-43.

[17] HU Yanjun, GHAFFAR A, HOU Yulong, et al. A micro structure POF relative humidity sensor modified with agarose based on surface plasmon resonance and evanescentwave loss[J]. Photonic Sensors, 2021, 11(4): 392-401.

[18] CAI Lu, WANG Jin, CHEN Maoqing, et al. A High-sensitivity strain sensor based on an unsymmetrical air-microbubble

Fabry-Pérot interferometer with an ultrathin wall[J]. Measurement, 2021, 181: 109651.
[19] ZHANG Peng, ZHU Yong, CHEN Weimin. A study on fourier transformation demodulating theory of the gap of iptical fiber Fabry-Pérot sensor[J]. Acta Photonica Sinica, 2004, 33(12): 1449-1452.
章鹏, 朱永, 陈伟民. 光纤法布里-珀罗传感器腔长的傅里叶变换解调原理研究[J]. 光子学报, 2004, 33(12): 1449-1452.
[20] NI Kai, CHAN Chichiu, CHEN Lihan, et al. A chitosan-coated humidity sensor based on Mach-Zehnder interferometer with waist-enlarged fusion bitapers[J]. Optical Fiber Technology, 2017, 33(59): 56-59.
[21] WANG Piaopiao, NI Kai, WANG Bowen, et al. Methylcellulose coated humidity sensor based on Michelson interferometer with thin-core fiber[J]. Sensors and Actuators A: Physical, 2019, 288: 75-78.
[22] GONG Tianyi, LIU Xiaoqi, WANG Zhi, et al. A highly sensitivity humidity sensor based on mismatching fused fiber Mach-Zehnder interferometric without moisture material coating[J]. Journal Optics, 2020, 22(2): 025801.
[23] TONG Ruijie, ZHAO Yong, ZHENG Hongkun, et al. Simultaneous measurement of temperature and relative humidity by compact Mach-Zehnder interferometer and Fabry-Pérot interferometer[J]. Measurement, 2020, 155: 107499.
[24] JI Peng, ZHU Meng, LIAO Changrui, et al. In-fiber polymer Microdisk resonator and its sensing applications of temperature and humidity[J]. ACS Applied Materials & Interfaces, 2021, 13(40): 48119-48126.
[25] LI Fei, LI Xuegang, ZHOU Xue, et al. Simultaneous measurement of temperature and relative humidity using cascaded C-shaped Fabry-Pérot interferometers[J]. Journal of Lightwave Technology, 2022, 40(4): 1209-1215.
[26] ZHANG Zhaoxu, GONG Huaping, YU Changgui, et al. Fiber optic Fabry-Pérot interferometer based on HA/PVA composite film for humidity sensing[J]. Optical Fiber Technology, 2022, 68: 102816.

High-sensitivity Fiber-optic Humidity Sensor without Sensitizing Material Modification

LI Mi, MA Chengju, LI Dongming, ZHANG Yuebin, BAO Shiqian, JIN Jiasheng, ZHANG Yao, LIU Qianzhen, LIU Ming, ZHANG Yixin
(*School of Science, Xi'an Shiyou University, Xi'an* 710065, *China*)

Abstract: Relative Humidity (RH) is a physical parameter which reflects the degree of atmospheric dryness. It has wide applications in agriculture, biology, petrochemical fields, food-processing, medical treatment and Internet of Things (IOT) technology. Fiber-optic humidity sensors have attracted widespread attention from scholars due to their high-measurement accuracy, anti-electromagnetic interference, multiplexing, and distributed sensing. Especially, humidity sensors based on Fabry-Pérot Interferometers (FPIs) have been widely valued for their high repeatability, compact size and high-sensitivity. Various humidity sensors based on silica fiber-optic have been reported. In the majority of fiber-optic humidity sensors, however, the sensitivity of RH detection can be improved by coating hygroscopic materials. At the same time, because they are fragile and inflexible, silica optical fibers must be treated carefully. This increases the cost and complexity of the fabrication process. Therefore, it has great research significance and application value to study new materials and structures. In order to simplify the manufacture of sensor and obtain excellent humidity sensitivity, a composite humidity sensor based on Polymethyl Methacrylate (PMMA)-microsphere and Single-mode Fiber (SMF) is designed and fabricated. Since the Polymer Optical Fiber (POF) material is very easily heated to form a molten state. In this work, the proposed sensor can be fabricated with an electric soldering iron. When the soldering iron is heated to about 70℃, place it 1 cm below the POF to slightly attach the POF to the SMF. Slowly rotate the heating source (i. e., electric iron) to allow the POF to be evenly heated. A Fabry-Pérot (F-P) cavity is formed between PMMA-microsphere and the fiber endface. It should be noted that adjusting the heat source temperature and distance between fiber-optic and heat source, the temperature of heating can be controlled in the heating process. Compared with the alcohol lamp heating method, the electric soldering iron heating method can provide a stable heating source and high safety factor in the experiment. And then, the humidity sensing characteristics of the sensor are theoretically and experimentally studied. When the external ambient humidity rises, the volume of PMMA-microsphere can expand after absorbing moisture from the surrounding. It causes the length of the F-P microcavity to grow. Then, the peak (or valley) of

the F-P reflection spectrum shift toward longer wavelengths (i.e., red-shift). Thus, the humidity sensing can be realized. To investigate the sensing performance of the designed sensor, a test system that includes a demodulator, a humidity box, and a personal computer is built. Firstly, humidity test experiments are performed when the RH increases from 30% to 80% at a step of 10%. The humidity experimental results show that the wavelength shifts approximately linearly with the humidity changing, and the linearity reaches 0.992 26. The sensitivity of the sensor is up to 173.36 pm/%RH in the humidity range of 30%~80%. Meanwhile, the sensor is placed in the temperature box (NBD-M1200-10IC, NOBODY. China). The reflection spectra of the sensor with different temperature are acquired by a spectral acquisition with the range of 1 520~1 580 nm. Experimental results demonstrate that the interference spectrum has a red-shifted about 3.15 nm in the temperature range from 35℃ to 65 ℃. The temperature sensitivity of the sensor is 105.07 pm/℃, and the linearity is 0.989 55. In the subsequent studies, we will consider cascading FBG in the proposed sensor to solve the problem that cross-sensitivity of temperature and humidity. Finally, the proposed sensor performs well, showing a superior stability and repeatability over the test cycles in the performance evaluation actualized. When relative humidity is 33%RH and 38%RH, the resonant wavelength of the reflection spectrum has a very small shift within 60 min. The maximum deviations are 0.08 nm and 0.09 nm, respectively. The results indicate that the proposed sensor can maintain good stability in a long-term working condition. In addition, the wavelength drift deviation of the three repeated experiments is small, and the sensitivities are 176.05 pm/%RH, 170.35 pm/%RH and 173.68 pm/%RH, respectively. The average humidity sensitivity of the three groups tests is 173.36 pm/%RH. The designed humidity sensor offers numerous advantages such as low cost, high-sensitivity, simple structure and easy fabrication, which has a wide application prospect in the field of biochemical, agriculture and environmental monitoring.

Key words: Fiber-optic sensor; Polymethyl methacrylate; Single-mode fiber; Fabry-Pérot cavity; Relative humidity

OCIS Codes: 060.2370; 160.5470; 060.2430; 120.2230

Foundation item: The Key Research and Development Plan Program of Shaanxi Province (No. 2018GY-062), the Innovation and Practice Ability Training Fund of Xian Shiyou University (No. YCS20213213)